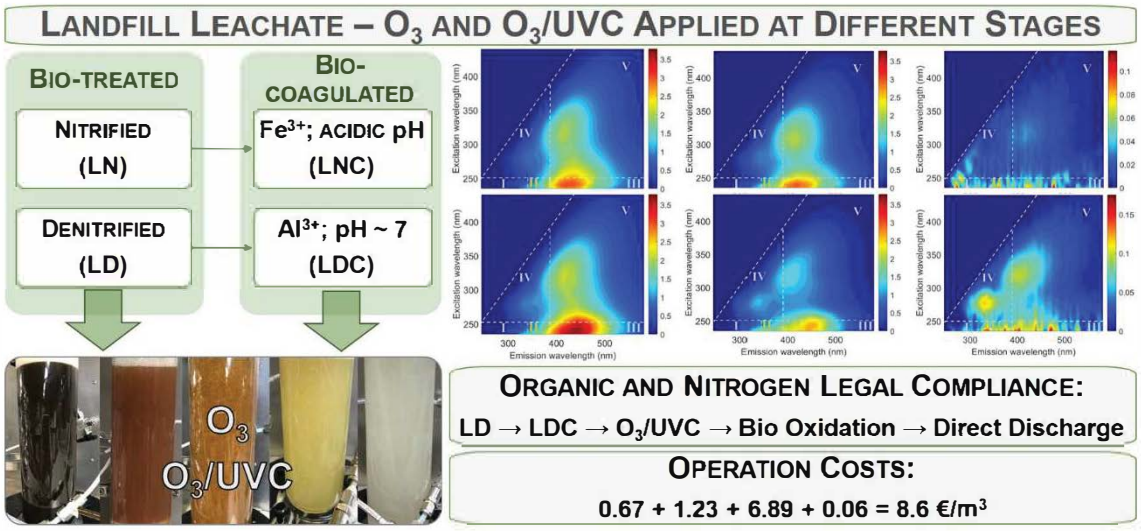
LANDFILL LEACHATE – O_3 AND O_3/UVC APPLIED AT DIFFERENT STAGES
BIO-TREATED
NITRIFIED (LN)
DENITRIFIED (LD)
BIO-COAGULATED
Fe^{3+}; ACIDIC pH (LNC)
Al^{3+}; pH ~ 7 (LDC)
O_3
O_3/UVC
Excitation wavelength (nm)
Emission wavelength (nm)
ORGANIC AND NITROGEN LEGAL COMPLIANCE:
LD → LDC → O_3/UVC → Bio Oxidation → Direct Discharge
OPERATION COSTS:
0.67 + 1.23 + 6.89 + 0.06 = 8.6 €/m³

How does the pre-treatment of landfill leachate impact the performance of O_3 and O_3/UVC processes?

Ana I. Gomes[1*], Bianca M. Souza-Chaves[2], Minkyu Park[2], Tânia F.C.V. Silva[1], Rui A.R. Boaventura[1], Vítor J.P. Vilar[1*]

[1]*Laboratory of Separation and Reaction Engineering-Laboratory of Catalysis and Materials (LSRE-LCM), Departamento de Engenharia Química, Faculdade de Engenharia da Universidade do Porto, Rua Dr. Roberto Frias, 4200-465 Porto, Portugal.*

[2]*Department of Chemical & Environmental Engineering, E, 1133 E James E Rogers Way, Harshbarger 108, Tucson, AZ 85721-0011, USA*

*Authors to whom correspondence should be addressed

Tel. +351 918257824; Fax: +351 225081674

E-mail addresses: ana.isabelgomes@fe.up.pt (Ana I. Gomes); vilar@fe.up.pt (Vítor J.P. Vilar)

Abstract

In this study, O_3 and O_3/UVC processes were evaluated for the treatment of landfill leachate after biological nitrification/denitrification, coagulation, or their combinations. The O_3-driven stage efficiency was assessed by the removal of color, organic matter (dissolved organic carbon (DOC) and chemical oxygen demand (COD)), and biodegradability increase (Zahn-Wellens test). Also, fluorescence excitation-emission matrix (EEM) and size exclusion chromatography coupled with OC detector (SEC-OCD) analyzes were carried out for each strategy. The bio-nitrified-leachate (L_N) was not efficiently mineralized during the O_3-driven processes since the high nitrites content consumed ozone rapidly. In turn, carbonate/bicarbonate ions impaired the oxidation of the bio-denitrified-leachate (L_D), scavenging hydroxyl radicals ($HO^{\bullet}$) and inhibiting the O_3 decomposition. For both bio-leachates, only O_3/UVC significantly enhanced the effluent biodegradability (>70%), but COD legal compliance was not reached. EEM and SEC-OCD results revealed differences in the organic matter composition between the nitrified-coagulated-leachate (L_{NC}) and denitrified-coagulated-leachate (L_{DC}). Nonetheless, the amount of DOC and COD removed per gram of ozone was similar for both. Cost estimation indicates the O_3-driven stage as the costliest among the treatment processes, while coagulation substantially reduced the cost of the following ozonation. Thus, the best treatment train strategy comprised L_{DC} (with methanol addition for denitrification and coagulated with 300 mg Al^{3+}/L, without pH adjustment), followed by O_3/UVC (transferred ozone dose of 2.1 g O_3/L and 12.2 kJ_{UVC}/L) and final biological oxidation, allowed legal compliance for direct discharge (for organic and nitrogen parameters) with an estimated cost of 8.9 €/m^3 (O_3/UVC stage counting for 6.9 €/m^3).

Keywords: Mature landfill leachate; Ozonation; UVC radiation; Biodegradability; Dissolved organic matter; Operating costs.

1. Introduction

Solid waste disposal in sanitary landfills is the most common method used worldwide for waste management (Kaza et al., 2018). An inevitable consequence of this practice is the generation of leachate, generally known as high-strength wastewater, particularly difficult to handle (Christensen et al., 1989; Renou et al., 2008). Leachate from mature landfills (> 10 years) is usually characterized by (Bhalla et al., 2013; Renou et al., 2008): (i) high ammonium content; (ii) low biodegradability; and (iii) high fraction of refractory and large organic molecules, such as humic and fulvic acids (also responsible for the typical leachate dark brown color). If not properly treated, the discharge of landfill leachate into the environment poses serious risks, as it may cause a deep impact on soil permeability and contamination of surface and groundwater (Vithanage et al., 2014).

Over the last decade, several research efforts have been made combining different treatment processes (biological and/or physicochemical) with advanced oxidation processes (AOPs) as a strategy to effectively treat landfill leachates, such as: (i) sequencing batch biofilm reactor (SBBR) + electro-Fenton (EF) (Zhang et al., 2014); (ii) activated sludge biological oxidation (ASBO) + coagulation/sedimentation (C/S) + EF, photo-Fenton (PF), or photo-electro-Fenton (PEF) (Moreira et al., 2015; Silva et al., 2017); (iii) SBB granular reactor + solar PF, electrolysis, H_2O_2, H_2O_2/UV or O_3 (Del Moro et al., 2016; Pastore et al., 2018); (iii) autotrophic nitrogen removal (ANR) combine with C/S, O_3 or Fenton, with pre- or post-treated by granular activated carbon (GAC) (Gao et al., 2015; Oloibiri et al., 2017a). However, those studies mainly target the removal of chemical oxygen demand (COD) and only few consider the nitrogen content (usually the ammonia content and not the total nitrogen (TN)). So, in view of simultaneous compliance for organic and nitrogen compounds legal parameters, V.

Vilar and co-workers proposed and tested a treatment train strategy that encompassed biological nitrification/denitrification, coagulation with iron salts at acidic pH, followed by PF oxidation and final biological oxidation (Gomes et al., 2019b; Silva et al., 2017). Also, a new artificial photoreactor (FluHelik) was developed for the advanced treatment of effluents with low transmissibility, like leachates. This strategy was tested at full-scale, where the FluHelik's design (4 photoreactors connected in series) enabled a flexible and compact solution for the photo-treatment of 20 m^3 of leachate and high performance was reported (Gomes et al., 2019a). Despite the promising results, some operational difficulties were highlighted regarding the PF stage, namely: (i) requires tight alkalinity control of the biological nitrification/denitrification stage; (ii) obliges the addition of chemicals, which may jeopardize compliance with legal discharge parameters (namely for sulfate ions and total iron); (iii) requires additional treatment time for iron-catalyst sedimentation; and (iv) produces iron-sludge. Considering these drawbacks, the usage of O_3-driven processes as an alternative to the PF stage was proposed.

Ozonation processes can be attractive for the treatment of landfill leachates, namely because ozone presents: (i) high oxidative power; (ii) great efficiency in color removal; (iii) high reactivity and selectivity towards electron-rich moieties of compounds; and (iv) the possibility to be combined with H_2O_2 and/or UVC radiation, which favors the production of hydroxyl radicals ($HO^{\bullet}$). These processes have been applied either to the raw leachate, mainly as a pre-treatment (Asaithambi et al., 2017; Cortez et al., 2011; Tizaoui et al., 2007), or later as a polishing step (Amaral-Silva et al., 2016; Cortez et al., 2010; Ntampou et al., 2006) prior to discharge in the environment. Beyond removing contaminants and reducing the organic load, several ozone-driven processes (O_3/UVC, O_3/H_2O_2, O_3/UVC/H_2O_2, catalytic or electro-catalytic-ozonation) have also proven to

enhance the biodegradability of landfill leachate (Ghahrchi and Rezaee, 2020; 2021). This is particularly relevant to outline a strategy for leachate treatment, as the combination of an ozone-driven process followed by a biological stage is expected to reduce the required ozone dose (thus, its costs) to reach legal compliance for direct discharge. In view of this, our previous research work (Gomes et al., 2020) focused on the application of different ozone-driven processes (O_3, O_3/UVC, O_3/H_2O_2 and O_3/UVC/H_2O_2), testing different initial pH values, ozone inlet concentrations, ozone rate flows and reactor system setups, on the treatment of a biologically nitrified and coagulated leachate. The main findings allowed to (i) establish the best operational conditions and system setup (in this case, a FluHelik coupled with a bubble column, with a Venturi injector at the inlet of the photoreactor); and (ii) demonstrate that the recalcitrant organic matter was successfully oxidized by O_3 and, in particular, by O_3/UVC, making it suitable for a following biological oxidation (both treatments reached COD values < 150 mg/L, Portuguese legal limit for direct discharge (236/98, 1998), at the end of a Zahn-Wellens biodegradability test). Although COD legal compliance was met, the high TN content (~0.56 g/L) of the leachate was not addressed, and many countries present regulatory limits for both parameters (Gomes et al., 2019b).

With the purpose to integrate an O_3-driven stage into a treatment train for mature urban landfill leachates and underlying compliance with legal discharge limits, this work investigates the performance of O_3 and O_3/UVC processes applied to leachate pre-treated with different technologies (including biological nitrogen removal and coagulation processes). The efficiency of the ozone-driven stage was evaluated by the removal of organic matter (in terms of dissolved organic carbon (DOC) and COD) and color, as well as by the ability to enhance the effluent biodegradability (in view of a complete treatment train containing a subsequent and final biological oxidation). For a

deeper understanding of the nature and fingerprints of the dissolved organic matter (DOM) in (treated) leachates, for each treatment strategy, the changes in the characteristics of organic matter in leachate samples were evaluated, by means of fluorescence excitation-emission matrix (EEM) spectroscopy and size exclusion chromatography coupled with organic carbon detector (SEC-OCD). Finally, estimations for the treatment costs considering 6 possible treatment train scenarios ((1) bio-nitrification + O_3/UVC + bio-denitrification; (2) bio-N removal + O_3/UVC + bio-oxidation, (3;4) bio-nitrification + iron-acidic coagulation (no nitrites) + O_3 or O_3/UVC + bio-denitrification, and (5;6) bio-N removal + aluminum-neutral coagulation + O_3 or O_3/UVC + bio-oxidation) were performed.

2. Materials and methods

2.1. Urban landfill leachate

The mature urban leachate used in this work was pre-treated by: (i) biological nitrification (L_N); (ii) biological nitrification/denitrification (L_D); (iii) biological nitrification followed by coagulation (L_{NC}); and (iv) biological nitrification/denitrification followed by coagulation (L_{DC}). The main physicochemical characteristics of each pre-treated leachate are presented in Table 1.

Insert Table 1

Both nitrified leachates (L_N and L_{NC}) were collected at a leachate treatment plant installed in a 20-year-old municipal landfill located in northern Portugal. L_N was collected after the aerated biological treatment stage (temperature and pH not controlled; hot air compressor and fine bubble aeration, 0.5 mg/L < dissolved oxygen < 1.0 mg/L, to promote nitrification), while L_{NC} was collected at the end of the following coagulation stage (coagulant dose of 240 mg Fe^{3+}/L and pH ~4). Both pre-treated

leachates were transported to the laboratory and stored at 4ºC until use. Before storage, L_{NC} was aerated (air pump at 3000 L/h, for 4h) for the conversion of nitrites to nitrates. In order to obtain the denitrified leachates (L_D and L_{DC}), part of the collected L_N was placed in a biological reactor (10 L capacity) with biomass previously adapted, under anoxic conditions and mechanical agitation, at room temperature (22-25ºC). Methanol was added as external carbon source for denitrification (2.5 mg CH_3OH/mg $N\text{-}NO_2^-$). After denitrification, part of L_D was used for coagulation tests with aluminum sulfate ($Al_2(SO_4)_3$), by means of *jar test*, without pH adjustment (further details can be found at *Supplementary Material* file).

2.2. Experimental setup

The lab-scale system consisted of a FluHelik photoreactor connected to a bubble column reactor ($Ø_{inner}$ = 73 mm; maximum fluid column height of 370 mm), with leachate recirculation (ISMATEC BVP-Z pump, flow rate (Q_l) of 75 L/h) amongst the reactors (Figure 1). The tests were conducted in semi-batch mode employing a Venturi to inject a continuous stream of O_3/O_2-gas mixture (ozone generator BMT 802N) upstream the photoreactor. The gaseous flow rate was regulated by a digital mass flow meter (Alicat Scientific). The ozone concentrations in the inlet and outlet of the system were measured (ozone analyser BMT 964), and the transferred ozone dose (OD_T) was calculated according to Eq. (1).

$$OD_T = \frac{Q_g}{V_L} \int_0^t \left(C_{O_3,I\text{-}g} - C_{O_3,O\text{-}g}\right) dt \qquad (1)$$

with OD_T (mg O_3/L effluent), calculated by integrating the difference between the constant inlet ozone concentration ($C_{O3,I\text{-}g}$) and the outlet/off-gas concentration ($C_{O3,O\text{-}g}$) during the applied time interval. Q_g (L/min) is the applied gas flow rate and V_L (L) is the volume of leachate in the reactor.

149 The ozone leaving the system was vented through a catalytic ozone destruction unit
150 (Heated Catalyst BMT) and bubbled into Woulff bottles containing 2% KI solution. For
151 the O_3/UVC process, a UVC lamp (Philips TUV 11W (bio-treated) or 6W (bio-
152 coagulated), model G6 T5, with the corresponding radiant power of 2.48 J/s and 1.7 J/s)
153 was placed inside the FluHelik.

154 *2.3. Experimental procedure*

155 In view of the proposed objectives, for each pre-treated leachate, experiments were
156 carried out with O_3 and O_3/UVC processes. All tests were performed using the
157 following experimental conditions: initial leachate pH of 9.0 (using NaOH), inlet ozone
158 dose of 18 mg O_3/min (inlet O_3 concentration set at 180 mg/L and gas flow rate at 0.1
159 L/min). Each treatment test was applied to 1.5 L of pre-treated leachate for (i) 12h and
160 10h, for O_3 and O_3/UVC processes, respectively, for LN and LD effluents; and (ii) 3h,
161 for all tests applied to L_{NC} and L_{DC}. During the tests, samples were collected
162 periodically for analytical characterization, at a sampling point located between the
163 FluHelik and the BC. To eliminate residual dissolved ozone, sample vials were
164 transferred to a water bath at 50 ºC, for 15 min.

165 *2.4. Analytical determinations*

166 Chloride (Cl^-), nitrite (NO_2^-), sulfate (SO_4^{2-}), and nitrate (NO_3^-) were quantified by ion
167 chromatography using a Dionex ICS-2100 apparatus. Heavy metals (Al, Cr, Cu, Fe, Ni
168 and Pb) were quantified by inductively coupled plasma optical emission spectrometry
169 (ICP-OES), using a Thermo iCAP 7000 equipment, after sample digestion with nitric
170 acid. The analysis of COD was made according to the dichromate closed reflux method
171 (Clesceri et al., 2005). The DOC determination was carried out using a Shimadzu TOC-
172 V_{CSN} analyzer (with previous filtration of the sample using 0.45 μm Nylon membrane
173 filters). The UV-Vis spectrum (after filtration and dilution) was measured in a scan

range of 200-600 nm (1 nm interval), using a UV-Vis spectrometer (VWR, UV-6300PC) and 1 cm quartz cuvette. Before and after each treatment stage the leachate's biodegradability was evaluated by the Zahn-Wellens test (OECD, 1992). Ultrapure and demineralized water were produced by a Millipore system (Direct-Q®) and a reverse osmosis system (Panice), respectively.

Fluorescence and absorbance spectra were measured using a Horiba Aqualog fluorometer. Fluorescence was scanned with excitation wavelengths from 225 to 450 nm in 5 nm increments and emission wavelengths from 250 to 580 nm in 1 nm increments. The inner filter was corrected using the measured absorbance spectra as described in Park and Snyder (2018). The regional integration and total fluorescence (TF) were calculated as described in Chen et al. (2003).

Dissolved organic matter (DOM) was characterized by size exclusion chromatography coupled with organic carbon detector (SEC-OCD) using a hydroxylated methacrylic polymer column (TOYOPEARL® HW-50S, Tosoh Bioscience LLC; 21 mm x 250 mm), high-performance liquid chromatography (HPLC) (Agilent 1290) hyphenated with an OCD (Suez GE Sievers M9 TOC analyzer).

2.5. Treatment cost analysis

For the biological stages, to estimate the energy cost for aeration and the cost of the external carbon donor, theoretical values for oxygen and COD consumption were employed. For the coagulation and ozone-driven stages, the operating costs were calculated taking into account the experimental conditions and data obtained, namely: (i) type and concentration of coagulant; (ii) amount of acid or base required for the pH adjustments; (iii) gas flow rate and ozone concentration and (iv) time required to achieve 85% (L_N and L_D) or 60% (L_{NC} and L_{DC}) of COD reduction (established according to the results obtained and calculated on the basis of the pseudo-first-order

rate constants). Furthermore, the following energy and reagents prices were considered: (i) 0.1276 €/kWh, energy market price in Portugal for industrial applications; (ii) 4.5 kg O_2/kWh for aeration carried out by fine bubble diffusers (Tchobanoglous et al., 2003); 15 kWh/kg O_3 for a corona discharge ozone generator fed with pure oxygen; (iv) 11W (L_N and L_D) or 6 W (L_{NC} and L_{DC}) for UVC lamp; (v) 0.48 €/kg for methanol; (vi) 0.08 €/m^3 for O_2; (vii) 0.24 €/kg for $FeCl_3$ 40% (w/w); (viii) 0.19 €/kg for $Al_2(SO_4)_3$ 48% (w/w), (ix) 0.16 €/kg for NaOH 30% (w/w), and (x) 0.10 €/kg for H_2SO_4 98% (w/w). Regarding the sludge treatment and disposal costs, based on previous work (Gomes et al., 2019a) an average value of 0.48 €/m^3 was assumed.

3. Results and discussion

3.1. Bio-treated leachate samples

According to the characteristics of the two bio-treated leachates (L_N and L_D) showed in Table 1, main differences are found for pH, inorganic carbon (DIC), and nitrogen content, which are related to the distinct biological metabolic processes involved in the nitrification and denitrification of the leachate. For biological nitrification (in this case partial nitrification, i.e., ammonium oxidation to nitrite), the autotrophic nitrifying bacteria consumed the inorganic carbon, thus reducing alkalinity and pH (theoretically, 7.14 mg of $CaCO_3$ are consumed per 1 mg of NH_4^+-N oxidized) (U.S.EPA, 1993). In turn, heterotrophic bacteria in biological denitrification recovered part of the inorganic carbon, which raises alkalinity and pH (theoretically, each mg of NO_2^--N reduced to N_2 causes an alkalinity increase of 3.57 mg $CaCO_3$) (U.S.EPA, 1993). Consequently, L_N effluent presents lower pH and DIC values, when compared to L_D, and the nitrogen content was mainly in the form of nitrite ions. Since L_D effluent resulted from denitrification of L_N, both presented similar concentration values for chloride and sulfate ions, as for some selected heavy metals (Table 1). Nonetheless, L_D effluent had

slightly higher DOC and COD values, most likely attributed to some remnants of biodegradable organic matter from the addition of the external carbon donor. This was supported by the Zahn-Wellens biodegradability test results.

3.1.1. Efficiency of the ozone-driven processes

Taking the above, the effect of the L_N and L_D distinct features on the performance of O_3 and O_3/UVC treatment was assessed. A first glance at the results (Table 2) suggests no significant differences between the efficiencies of the ozone-driven processes applied to L_N and L_D. For both bio-treated leachates, DOC and COD removals were very similar at the end of the ozonation treatment. Also, the combination of O_3/UVC further increased the organic matter oxidation, with L_D presenting 10% less mineralization than L_N. A closer look at the organic matter removal profiles (Fig. 2) reveals specific features during the ozone-based treatments.

Insert Table 2

For L_N, there was an initial period up to about 7h, for O_3, and 5h, for O_3/UVC (corresponding to OD_T of 5.0 and 3.6 g O_3/L, respectively), in which practically no mineralization was observed (Fig. 2 (a.1) and (a.2)). This induction period coincided with the oxidation of nitrites to nitrates ($NO_2^- + O_3 \rightarrow NO_3^- + O_2$, k = 1.8 $\times 10^5$ M^{-1} s^{-1} (Hoigné et al., 1985), k = 5.8 $\times 10^5$ M^{-1} s^{-1} (Liu et al., 2001)) and did not appear to affect COD reduction. A clear linear relation was obtained between the OD_T and the amount of nitrites oxidized (see *Supplementary Material*, Fig. SM-2), with an expected highest rate found for O_3/UVC treatment. This high ozone consumption hindered mineralization that started as soon as all the nitrite was converted to nitrate. Afterward and until the end of the tests, the DOC reduction profile was followed by a significant drop in pH (down to pH 3.2 and 5.6 for O_3-only and O_3/UVC treatments, respectively, Fig. 2 (b.1) and (b.2)). This acidification may be associated with the oxidation of

complex organic compounds in the leachate with the expected formation of carboxylic acids (Chys et al., 2015; Tizaoui et al., 2007), and with carbon dioxide and carbonic acids resulting from the mineralization of organic compounds. It is known that pH influences the oxidation pathways for ozonation processes (higher pH decomposes ozone more rapidly, since hydroxide ion (OH^-) is an initiator of the reaction chain described in Equations 1 to 7, thus producing a greater amount of $HO^\bullet$ radicals (Gardoni et al., 2012)) and also plays an important role by influencing the concentrations of the dissociated/non-dissociated forms of the leachate components. So, it is interesting to note that the mineralization kinetic constants (k, min^{-1}) obtained for L_N became higher when its buffer capacity was lost. This indicates that other mechanisms were occurring in the medium, generating reactive species and contributing to the oxidation of the organic matter. For instance, although (as mentioned) O_3 reacts with nitrite mainly to form nitrate, peroxynitrite (2.6%) and $HO^\bullet$ radicals (~ 8%) are also generated, and 50% of peroxynitrite (stable at high pH) potentially gives rise to further $HO^\bullet$ radicals when the pH decreases to near neutral conditions (Naumov et al., 2010). Furthermore, in the presence of UVC radiation, ozone is photolyzed to form hydrogen peroxide (H_2O_2), which can itself be photolyzed generating $HO^\bullet$ radicals or act as an initiator for the ozone chain reaction mechanism to form $HO^\bullet$ radicals (Equations 8 to 10).

$$O_3 + OH^- \rightarrow O_2 + HO_2^- \quad \text{(O transfer)} \quad k_1 = 70\ M^{-1}\ s^{-1} \qquad (1)$$

$$O_3 + HO_2^- \rightarrow O_3^{\bullet -} + HO_2^\bullet \quad (e^- \text{ transfer}) \quad k_2 = 2.8\times10^6\ M^{-1}\ s^{-1} \qquad (2)$$

$$HO_2^\bullet \leftrightarrow O_2^{\bullet -} + H^+ \quad k_3 = 3.2\times10^5\ M^{-1}\ s^{-1};\ k_{-3} = 2.0\times10^{10}\ M^{-1}\ s^{-1} \qquad (3)$$

$$O_2^{\bullet -} + O_3 \rightarrow O_3^{\bullet -} + O_2 \quad k_4 = 1.6\times10^9\ M^{-1}\ s^{-1} \qquad (4)$$

$$O_3^{\bullet -} + H^+ \leftrightarrow HO_3^\bullet \quad k_5 = 5.2\times10^{10}\ M^{-1}\ s^{-1};\ k_{-5} = 3.3\times10^2\ M^{-1}\ s^{-1} \qquad (5)$$

$$HO_3^\bullet \rightarrow {}^\bullet OH + O_2 \quad k_6 = 1.1\times10^5\ M^{-1}\ s^{-1} \qquad (6)$$

$$O_3^{\bullet -} + {}^\bullet OH \rightarrow O_3 + OH^- \quad k_7 = 2.5\times10^9\ M^{-1}\ s^{-1} \qquad (7)$$

$$O_3 + H_2O + h\nu \rightarrow H_2O_2 + O_2 \quad (h\nu < 300\ nm) \quad (8)$$

$$H_2O_2 + h\nu \rightarrow 2OH^{\bullet} \quad (\phi_{OH^{\bullet}} = 1) \quad (9)$$

$$O_3 + H_2O_2 \rightarrow HO_2^{\bullet} + OH^{\bullet} + O_2 \quad k_{10} = 6.5\times10^{-2}\ M^{-1}\ s^{-1} \quad (10)$$

Insert Figure 2

Although the DOC and COD removal of L_N and L_D at the longest exposure time were similar to each other, L_D exhibited higher attenuation for both parameters at earlier exposure times. This trend in the treatment of L_D, when compared to L_N, can be justified by (1) absence of nitrites (avoiding ozone consumption for nitrites oxidation into nitrates during the first hours of treatment, making it available for organic matter oxidation) and (2) pH buffer effect due to the higher alkalinity content (observed by the less pronounced pH decay, Fig.1 (b.1) and (b.2)). The latter can cause both positive and negative impacts on mineralization efficiency during ozonation. On the one hand, L_D alkalinity allowed to maintain higher pH values throughout the treatments (particularly for O_3/UVC), thus promoting the autocatalytic reaction that produces $HO^{\bullet}$ radicals, strong and non-specific oxidants that are responsible for mineralization (Gardoni et al., 2012; Rosenfeldt et al., 2006); on the other hand, it is known that carbonate and bicarbonate ions may act as $HO^{\bullet}$ scavengers (as described in Equations 11 and 12), hindering the organic matter oxidation (Miklos et al., 2018), and also as “inhibitors” in the O_3 decomposition (Elovitz et al., 2000).

$$HCO_3^{\bullet -} + {}^{\bullet}OH \rightarrow CO_3^{\bullet -} + H_2O \quad k_{11} = 8.5\times10^{6}\ M^{-1}\ s^{-1} \quad (11)$$

$$CO_3^{2-} + {}^{\bullet}OH \rightarrow OH^{-} + CO_3^{\bullet -} \quad k_{12} = 4.2\times10^{8}\ M^{-1}\ s^{-1} \quad (12)$$

Ozone effectively reacts with chromophores. This was clearly seen by the color evolution during the first hour of treatment (see Fig. SM-3). At the end of the ozone-driven treatments, the intense brown color presented by both bio-treated leachate decreased to a very slight yellow. The color values (for a 1:20 dilution) obtained at the

end of the treatments by O_3 and O_3/UVC were, respectively, 28 and 9 units of Pt-Co, for L_N, and 30 and 20 units of Pt-Co, for L_D. Another indicator that can be employed to assess the effectiveness of ozone-driven processes is the change in biodegradability (Chen et al., 2019). Therefore, prior to and after the ozonation treatments, the biodegradability of each leachate was evaluated by the Zahn-Wellens 28-day test and the following results were obtained: (i) L_N = 7%, after O_3 = 51% and O_3/UVC = 73%; and (ii) L_D = 11%, after O_3 = 69% and O_3/UVC = 80%. Bearing in mind that for the effluent to be considered biodegradable, the organic carbon content must decrease by 70% after the 28-day test (Pluciennik-Koropczuk and Myszograj, 2018; Silva et al., 2013), for both bio-treated leachates, this only occurred after treatment with O_3/UVC. Also, in view of a target COD value < 150 mg/L (the legal limit for direct discharge), it is worth to mention that, in spite not achieved for any of the tested conditions, for the O_3/UVC treatments, COD values of 205 and 167 mg/L were reached at the end of the biodegradability tests for L_N and L_D, respectively. Therefore, the treatment of bio-treated leachate with O_3 alone will be disregarded as a possible treatment strategy.

3.1.2. Organic matter characterization

According to Chen et al. (2003), the fluorescence spectrum can be divided into five regions based on the type and location of fluorescent material: (i) region I – tyrosine-like aromatic protein (Ex < 250 nm, Em < 330 nm); (ii) region II – tryptophane-like aromatic protein (Ex < 250 nm, 330 nm < Em < 380 nm); (iii) region III – fulvic-like acids (Ex < 250 nm, Em > 380 nm); (iv) region IV – soluble microbial metabolic by-products (Ex > 250 nm, Em < 380 nm) and (v) region V – humic-like acids (Ex > 250 nm, Em > 380 nm). Figure 3a shows the relative fluorescence intensities integrated at each fluorescent region. A similar distribution of relative fluorescence was observed for L_N and L_D, inferring similar physicochemical characteristics of fluorophores. This can

be expected as L_D was obtained from the biological denitrification of L_N effluent. For both bio-treated effluents, 3D-EEM contours (Fig. 3 (b.1) and (b.2)) highlight two main regions responsible for more than 60% of total fluorescence intensity: (i) the fulvic acid-like matter (region III), representing 31.0% (L_N) and 33.5% (L_D), and (ii) humic acid-like matter (region V), corresponding to 35.5% (L_N) and 33.1% (L_D). This high fraction of fulvic- and humic-like acids is also an indication of the chemical stability of the leachate (Oloibiri et al., 2017b).

Insert Figure 3

After O_3/UVC treatment, the total fluorescence intensity largely decreased (95% and 92% for L_N and L_D, respectively), but major differences can be visualized in the 3D-EEM for both tested leachates (Fig. 3 (b.1') and (b.2')). While for the L_N, the fulvic- and humic-like matter regions remained with high fluorescence (30.8% and 39.1%, respectively, of the total fluorescence), for L_D, the fluorescence of those regions significantly decreased. The region with greater fluorescence intensity (representing 31.2% of the total fluorescence) was related to soluble microbial by product-like matter (region IV). Furthermore, for L_D, after O_3/UVC treatment, there was an increase of fluorescence related to protein-like substances (contrary to the treated L_N), with regions I and II counting for 36.3% of the total fluorescence. Together, these features of the treated L_D are likely responsible for its higher biodegradability.

Size exclusion chromatography combined with organic carbon detection (SEC-OCD) is a well-proven method for separating the poll of DOM into main fractions of different sizes and chemical functions and quantifying these on the basis of organic carbon (Huber et al., 2011). Observing the SEC-OCD chromatograms (Fig. 3 (c)), for both bio-treated leachates it is possible to verify the predominance of humic substances, with no noticeable peaks for lower molecular weight matter, such as building blocks and low

molecular weight acids/neutrals. After O_3/UVC treatment, the peak area related to humic substances decreased significantly, particularly for L_D (72.7% decay *vs.* 58.9% for L_N). Also, there was a shift of retention time at which the maximum OCD intensity was observed, suggesting lower molecular weight of the humic substances remaining.

3.2 Bio-coagulated leachates

The bio-coagulated leachates (L_{NC} and L_{DC}) were coagulated, considering the distinct characteristics of their corresponding bio-treated leachates (Table 1). L_N presents low alkalinity (as discussed above), which allows its acidification (i.e., sulfuric acid addition) without compromising the discharge limit for sulfate ions (Table 1). So, as proposed by different authors (Amokrane et al., 1997; Castrillón et al., 2010; Daud et al., 2012; Vedrenne et al., 2012) and tested on previous works with this type of leachate (Gomes et al., 2019a; Gomes et al., 2019b; Silva et al., 2017), L_{NC} results from coagulation using ferric salts at acidic conditions (240 mg Fe^{3+}/L and pH ~4). Attention should be drawn that the L_{NC} effluent was collected in the landfill plant and does not correspond to the direct coagulation of the L_N used for testing. Nonetheless, from previous coagulation tests under similar conditions, also using nitrified leachate from the same landfill (Gomes et al., 2019a; Silva et al., 2017), the performance of the coagulation stage to obtain L_{NC} can be assumed between 47% to 60% removal for both DOC and COD parameters. Note that aeration was afterward applied to oxidize nitrites to nitrates (Table 1), eliminating its interference in the ozonation reactions towards the bio-recalcitrant organic content of the L_{NC}.

In turn, to take advantage of the basic pH and buffering capacity (due to the recovery of alkalinity by bio-denitrification) of L_D, and to attain a final coagulated effluent with near-neutral pH conditions, coagulation with aluminum salts at natural pH was tested. Considering the *jar-test* results (Table SM-1) and the sulfate legal limit compliance (due

374 to the addition of $Al_2(SO_4)_3$ as coagulant), a coagulant dose of 300 mg Al^{3+}/L was
375 selected. Using the natural pH of the L_D effluent, the selected coagulant dose allowed
376 50.5% and 54.4% of DOC and COD removal, 63.3% of turbidity reduction, and a final
377 pH of 6.2 (Table SM-1).
378 *3.2.1. Efficiency of the ozone-driven processes*
379 For L_{NC}, as a result of the absence of nitrites, more oxidant species were available to
380 react with the organic matter and, unlike L_N, not only COD but also DOC has decreased
381 continuously since the beginning of the ozone-driven treatments (Fig. 4 (a.1) and (a.2)).
382 Additionally, for both O_3 and O_3/UVC treatments, the L_{NC} presented higher percentages
383 of DOC and COD removal when compared to the L_{DC} (Table 2). However, it can be
384 misleading, as attention should be given to the differences of the organic content
385 between the bio-coagulated leachates (lower organic content of L_{NC} when compared to
386 L_{DC}, see Table 1). Thus, although L_{NC} presents higher pseudo-first-order rate constants
387 (k, min^{-1}) for DOC and COD removal, it is possible to verify that the amount of DOC
388 and COD removed per gram of ozone is very similar for both bio-coagulated leachate
389 effluents. This feature was valid for the two ozone-driven processes tested. For the bio-
390 treated leachates, the pH decay for L_{DC} was less pronounced due to its higher alkalinity
391 content (buffer effect) (Fig. 4 (b.1) and (b.2)). Also, for both bio-coagulated leachates,
392 pH decay was lower for the O_3/UVC process.
393 **Insert Figure 4**
394 The color values (for a 1:20 dilution) obtained at the end of the treatments (3h) by O_3
395 and O_3/UVC were, respectively, 13 and 9 units of Pt-Co, for L_{NC}, and 12 and 9 units of
396 Pt-Co, for L_{DC} (Fig. SM-5). In respect to the biodegradability before and after ozone-
397 driven treatments, the following results were obtained: (i) L_{NC} = 17%, and after O_3 =
398 81% and O_3/UVC = 93%; and (ii) L_{DC} = 19%, and after O_3 = 83% and O_3/UVC = 87%

399 (Table 1 and 2). Moreover, the COD values at the end of the Zahn-Wellens test were for
400 L_{NC} of 123 mg/L (O_3) and 22 mg/L (O_3/UVC), and for L_{DC} of 174 mg/L (O_3) and 144
401 mg/L (O_3/UVC). In retrospect, except for O_3 applied to L_{DC}, all treatment scenarios
402 reached a final COD < 150 mg/L at the end of the biodegradability test.

403 *3.2.2 Organic matter characterization*

404 The coagulation stage reduced total fluorescence intensity by 61.5% and 60.3% for the
405 nitrified and denitrified leachate, respectively (to discussion, L_{NC} will be assumed as
406 resulting from the coagulation of L_N). Concerning the fluorescence intensity by region
407 (I to V), there was a decrease of 46%, 54%, 63%, 58% and 67%, from L_N to L_{NC}, and
408 25%, 48%, 65%, 49% and 71%, from L_D to L_{DC} (Table SM-2). Despite the similarity in
409 the fluorescence intensity decline (either total or by region, except for region I), as a
410 result of the distinct biological and coagulation processes, different 3D-EEM patterns
411 were obtained for the L_{NC} and L_{DC} effluents (Fig. 5 (b.1) and (b.2)). Aftab and Hur
412 (2017) also reported higher removal of the humic-like (75%) versus the fulvic-like (~
413 58%) acids for a coagulation treatment with an optimized dose of 300 mg Al^{3+}/L. The
414 much lower removal of tyrosine-like protein (region I) was also verified in other studies
415 (Aftab et al., 2020; Wassink et al., 2011), having been attributed to the smaller
416 molecular size of these compounds.

417 **Insert Figure 5**

418 For L_{NC}, after O_3 and O_3/UVC treatment, total fluorescence intensity was reduced by
419 98.1% and 98.7%, respectively (Table SM-2). In both ozone-driven treatments, but
420 more pronounced in O_3/UVC, the relative fluorescence intensity decreased (Fig. 5 (a.1))
421 in the regions associated with fulvic- and humic-like matter (from 60.2% to 48.1% after
422 O_3, and to 38.9% after O_3/UVC), and increased in the regions related to tyrosine-like
423 protein and microbial by-products (from 14.3% to 35.5% after O_3, and to 44.6% after

424 O_3/UVC). Those regions (I and IV) reflect bioavailable substrates (Henderson et al.,
425 2009; Hudson et al., 2007), presenting a strong correlation with BOD_5 (Yang et al.,
426 2013). These changes in DOM composition are in line with the results obtained in the
427 Zahn-Wellens biodegradability tests. By applying coagulation/ozonation to treat
428 membrane concentrates from landfill leachate, Chen et al. (2019) observed similar
429 fluorescence trends and proposed that protein-like matter was produced as intermediates
430 of the degradation of fulvic-like substances in the ozonation process, thereby producing
431 an effluent suitable for a subsequent biological oxidation treatment stage.
432 In respect to L_{DC}, total fluorescence intensity decreased 90.2% and 96.4% (Table SM-
433 2), respectively, after O_3 and O_3/UVC oxidation. Analysing the relative fluorescence
434 (Fig. 5 (a.2)), the application of O_3 did not significantly change the proportions of
435 fulvic- and humic-like acids (in fact, there was a slight increase from 53.5% to 56.7%).
436 In turn, after O_3/UVC treatment, not only the proportion of regions III and V in total
437 fluorescence decreased, but also there was a significant increase (nearly two-fold) of the
438 relative fluorescence intensity for tyrosine-like protein and microbial by-products.
439 Again, these results are in good agreement with the observed by Chen et al. (2019) and
440 with the biodegradability increase revealed by the Zahn-Wellens tests.
441 SEC-OCD chromatograms reveal once more the predominance of humic substances,
442 with coagulation shifting humic peaks towards later retention time when compared to
443 the respective bio-treated effluents (comparison between Fig. 3 (c) and Fig. 5 (c)). This
444 indicates that coagulation not only reduced the organic carbon (peak area decrease of
445 52.7% and 69.7%, respectively for L_{NC} and L_{DC}) but also removed the relatively high
446 molecular weight humic matter, which is known to be carboxylic-rich. For L_{NC} effluent,
447 a peak area reduction of 87.2% and 91.1% were obtained for both ozone-driven
448 treatments, with humic substances peak slightly changing to earlier retention time after

449 O_3-only. In turn, for L_{DC} treated by O_3, not only the humic substances peak changed
450 significantly to earlier retention time, suggesting higher molecular weight of the organic
451 matter, but also the peak area only decreased 13.4%. The poor performance of O_3
452 treatment was partially overcome by its combination with UVC radiation, with a
453 decrease of the humic substances peak area of 66.9% (but still 20% lower than those
454 obtained for L_{NC}).

455 *3.3. Treatment costs evaluation*

456 In view of simultaneous legal compliance for organic and nitrogen compounds, 6
457 possible treatment train strategies were evaluated in terms of operating costs (Table 3):
458 (1) bio-nitrification + O_3/UVC + bio-denitrification; (2) bio-N removal + O_3/UVC +
459 bio-oxidation; (3,4) bio-nitrification + iron-acidic coagulation (no nitrites) + O_3 or
460 O_3/UVC + bio-denitrification; and (5,6) bio-N removal + aluminum-neutral coagulation
461 + O_3 or O_3/UVC + bio-oxidation).

462 **Insert Table 3**

463 Ozone-driven treatment stage is the most expensive among the tested unit treatment
464 processes (Table 3). Coagulation substantially reduced the cost associated with the
465 subsequent ozone process. Accordingly, the treatment trains without coagulation (no. 1
466 and no. 2) were not economically viable. Regarding L_N, if full nitrification (i.e., bio-
467 oxidation of nitrite into nitrate) had occurred in the first biological reactor, it would be
468 possible to expect a cost-reduction of ~40% for the O_3-driven stage (to 20.5 €/m^3, but
469 still not economically viable). As coagulation promotes a significant reduction of the
470 leachate organic load (~50%), the required ozone dose to achieve a biodegradable
471 effluent, able to reach COD < 150 mg/L after a subsequent biological oxidation step, is
472 significantly lower; thus operational costs are substantially reduced (treatment trains
473 no.3 to 6). Considering the bio-coagulation pre-treatments, the strategies with L_{NC}

474 presented the lowest operational costs (Table 3), particularly when the O_3/UVC
475 advanced oxidation process is applied (as it showed the highest pseudo-first-order rate
476 constant for COD removal, Table 2). Nonetheless, knowing that only partial
477 nitrification occurs in the 1st biological reactor and, from previous experiences using
478 similar bio-nitrified leachate and coagulation conditions (Gomes et al., 2019a; Gomes et
479 al., 2019b; Silva et al., 2017), at the end of the C/S stage, the leachate still presents part
480 of the nitrogen content in the nitrite form (~ 70%). This is not desirable, as the presence
481 of nitrites in downstream advanced stage oxidation will inevitably lead to an increase in
482 costs (to 9.4 and 12.3 €/m^3, for the O_3 process, considering leachate with 500 and 1000
483 mg N/L of nitrite before coagulation). Therefore, the biological nitrogen removal should
484 preferentially be performed at the first biological stage (strategies no. 5 and no. 6).
485 Taking the reported costs (between 10 to 25 €/m^3 (Gomes, 2020)) of landfills in
486 Portugal whose leachate treatment complies with the legal limits for direct discharge
487 into the environment (by means of reverse osmosis process), treatment train strategy no.
488 6 may be considered economically competitive. Furthermore, the problems arising from
489 the concentrate that results from reverse osmosis are absent in ozone-based processes.

490 **4. Conclusions**

491 The performance of O_3 and O_3/UVC processes applied to urban mature leachate pre-
492 treated with different technologies, the ability to comply with the legal limits for direct
493 discharge into the environment, and the economic viability of different treatment trains,
494 were evaluated in this work. In the absence of a coagulation stage, both bio-treated
495 leachates (L_N and L_D) required an ozone dose (OD_T) of 7.1 g O_3/L combined with 59.5
496 kJ/L of UVC radiation, to obtain a biodegradable effluent. However, it is not certain that
497 after a subsequent biological treatment, the COD target value is attained, and the
498 treatment cost exceeds 30 €/m^3. Therefore, the inclusion of a chemical coagulation

process before the ozone-driven stage shows to be essential for the economic feasibility of a treatment train. The changes in DOM composition over the various treatment stages tested were consistent with the biodegradability presented by the respective effluents and showed that the degradation of fulvic- and humic-like matter by ozone-driven processes increases the content of the protein-like substance.

To deal with mature urban landfill leachate, among the various treatment train strategies proposed, the most suitable is as follows: (i) first biological stage for nitrification/denitrification (with the addition of an external carbon source), followed by (ii) coagulation, without pH adjustment and using 300 mg Al^{3+}/L, and (iii) advanced oxidation by means of O_3/UVC up to OD_T of 2.1 g O_3/L and 12.2 kJ_{UVC}/L, prior to (iv) final biological oxidation. This sequence allows reaching a final effluent able to simultaneously comply with the legal discharge values for organic and nitrogen parameters, and for other parameters whose concentration increases with the addition of chemicals along the treatment train (such as sulfate ions and total iron). Furthermore, the operational cost for this treatment train is expected to be 8.9 €/m^3, with O_3/UVC process counting for 6.9 €/m^3, which is reasonable considering the costs for current membrane technology (10 to 25 €/m^3).

Acknowledgements

The financial support for this work results from: (i) project "AIProcMat@N2020 - Advanced Industrial Processes and Materials for a Sustainable Northern Region of Portugal 2020" (ref. NORTE-01-0145-FEDER-000006) financed by Norte Portugal Regional Operational Programme (NORTE2020), under the Portugal 2020 Partnership Agreement, through the European Regional Development Fund (ERDF); (ii) Associate Laboratory LSRE-LCM base funding (UIDB/50020/2020), supported by Portuguese funds through FCT/MCTES (PIDDAC). Ana I. Gomes acknowledges her Ph.D.

524 scholarship (PD/BD/105980/2014) financed by FCT. Tânia F.C.V. Silva and Vítor J.P.
525 Vilar acknowledge the FCT Individual Call to Scientific Employment Stimulus 2017
526 (CEECIND/01386/2017 and CEECIND/01317/2017, respectively).
527

528 **References**

529 Decree-Law no. 236/98, 1998, Portuguese Republic Diary - I Series - A.

530 OECD, 1992 OECD Guideline for Testing of Chemicals, Test No. 302B: Inherent
531 Biodegrdability: Zahn-Wellens/EMPA test.

532 Aftab, B., Cho, J., Shin, H.S. and Hur, J. 2020. Using EEM-PARAFAC to probe NF
533 membrane fouling potential of stabilized landfill leachate pretreated by various
534 options. Waste Manage. 102, 260-269.

535 Aftab, B. and Hur, J. 2017. Fast tracking the molecular weight changes of humic
536 substances in coagulation/flocculation processes via fluorescence EEM-
537 PARAFAC. Chemosphere 178, 317-324.

538 Amaral-Silva, N., Martins, R.C., Castro-Silva, S. and Quinta-Ferreira, R.M. 2016.
539 Ozonation and perozonation on the biodegradability improvement of landfill
540 leachate. J. Environ. Chem. Eng. 4, 527-533.

541 Amokrane, A., Comel, C. and Veron, J. 1997. Landfill leachates pretreatment by
542 coagulation/flocculation. Water Resour. 31(11), 2775-2782.

543 Asaithambi, P., Sajjadi, B., Aziz, A.R.A. and Daud, W.M.A.B.W. 2017. Ozone (O_3)
544 and sono (US) based advanced oxidation processes for the removal of color,
545 COD and determination of electrical energy from landfill leachate. Sep. Purif.
546 Technol. 172, 442-449.

547 Bhalla, B., Saini, M.S. and Jha, M.K. 2013. Effect of age and seasonal variations on
548 leachate characteristics of municipal solid waste landfill. Int. J. Res. Eng.
549 Technol. 02, 223-232.

550 Castrillón, L., Fernández-Nava, Y., Ulmanu, M., Anger, I. and Maraños, E. 2010.
551 Physicochemical and biological treatment of MSW landfill leachate. Waste
552 Manage. 2010(30), 228-235.

553 Chen, W., Gu, Z., Wen, P. and Li, Q. 2019. Degradation of refractory organic
554 contaminants in membrane concentrates from landfill leachate by a combined
555 coagulation-ozonation process. Chemosphere 217, 411-422.

556 Chen, W., Westerhoff, P., Leenheer, J.A. and Booksh, K. 2003. Fluorescence
557 Excitation-Emission matrix regional integration to quantify spectra for dissolved
558 organic matter. Environ. Sci. Technol. 37, 5701-5710.

559 Christensen, T., Cossu, R. and Stegmann, R. (1989) Sanitary landfilling: Process,
560 technology and environmental impact, Academic Press Limited, London.

561 Chys, M., Oloibiri, V., Audenaert, W.T.M., Demeestere, K. and Van Hulle, S.W.H.
562 2015. Ozonation of biologically treated landfill leachate: efficiency and insights
563 in organic conversions. Chem. Eng. J. 277(1), 104-111.

564 Clesceri, L.S., Greenberg, A.E. and Eaton, A.D. (2005) Standard Methods for
565 Examination of Water & Wastewater, American Public Health Association
566 (APHA), American Water Works Association (AWWA) & Water Environment
567 Federation (WEF).

568 Cortez, S., Teixeira, P., Oliveira, R. and Mota, M. 2010. Ozonation as polishing
569 treatment of mature landfill leachate. J. Hazard. Mater. 182(1-3), 730-734.

570 Cortez, S., Teixeira, P., Oliveira, R. and Mota, M. 2011. Evaluation of Fenton and
571 ozone-based advanced oxidation processes as mature landfill leachate pre-
572 treatments. J. Environ. Manage. 92, 749-755.

573 Daud, Z., Latif, A.A.A. and Rui, L.M. 2012. Coagulation-flocculation in leachate
574 treatment by using ferric chloride and alum as coagulant. Int. J. Eng. Res. Appl.
575 2(4), 1929-1934.

576 Del Moro, G., Prieto-Rodríguez, L., De Sanctis, M., Di Iaconi, C., Malato, S. and
577 Mascolo, G. 2016. Landfill leachate treatment: comparison of standalone
578 electrochemical degradation and combined with a novel biofilter. Chem. Eng. J.
579 288, 87-98.

580 Elovitz, M.S., von Gunten, U. and Kaiser, H.-P. 2000. Hydroxyl Radical/Ozone Ratios
581 During Ozonation Processes. II. The Effect of Temperature, pH, Alkalinity, and
582 DOM Properties. Ozone Sci. Eng. 22(2), 123-150.

583 Gao, J., Oloibiri, V., Chys, M., De Wandel, S., Decostere, B., Audenaert, W.T.M., He,
584 Y.L. and Van Hulle, S.W.H. 2015. Integration of autotrophic nitrogen removal,
585 ozonation and activated carbon filtration for treatment of landfill leachate.
586 Chem. Eng. J. 275, 281-287.

587 Gardoni, D., Vailati, A. and Canziani, R. 2012. Decay of ozone in water: A review.
588 Ozone Sci. Eng. 34(4), 233-242.

589 Ghahrchi, M. and Rezaee, A. 2020. Electro-catalytic ozonation for improving the
590 biodegradability of mature landfill leachate. J. Environ. Manage. 254, 109811.

591 Ghahrchi, M. and Rezaee, A. 2021. Electrocatalytic ozonation process supplemented
592 by EDTA-Fe complex for improving the mature landfill leachate treatment.
593 Chemosphere 263, 127858.

594 Gomes, A.I. (2020) Treatment train for mature urban landfill leachate, Faculty of
595 Engineering, University of Porto.

596 Gomes, A.I., Foco, M.L.R., Vieira, E., Cassidy, J., Silva, T.F.C.V., Fonseca, A.,
597 Saraiva, I., Boaventura, R.A.R. and Vilar, V.J.P. 2019a. Multistage treatment
598 technology for leachate from mature urban landfill: Full scale operation
599 perfomance and challenges. Chem. Eng. J. 376, 120573.

600 Gomes, A.I., Santos, S.G.S., Silva, T.F.C.V., Boaventura, R.A.R. and Vilar, V.J.P.
601 2019b. Treatment train for mature landfill leachates: Optimization studies. Sci.
602 Total Environ. 673, 470-479.

603 Gomes, A.I., Soares, T.F., Silva, T.F.C.V., Boaventura, R.A.R. and Vilar, V.J.P. 2020.
604 Ozone-driven processes for mature urban landfill leachate treatment: Organic
605 matter degradations, biodegradability enhancement and treatment costs for
606 different reactors configuration. Sci. Total Environ. 724, 138083.

607 Henderson, R.K., Baker, A., Murphy, K.R., Hambly, A., Stuetz, R.M. and Khan, S.J.
608 2009. Fluorescence as a potential monitoring tool for recycled water systems: a
609 review. Water Res. 43, 863-881.

610 Hoigné, J., Bader, H., Haag, W.R. and Staehelin, J. 1985. Rate constants of reactions
611 of ozone with organic and inorganic compounds in water III. Inorganic
612 compounds and radicals. Water Res. 19, 993-1004.

613 Huber, S.A., Balz, A., Abert, M. and Pronk, W. 2011. Characterisation of aquatic
614 humic and non-humic matter with size-exclusion chromatography - organic
615 carbon detection - organic nitrogen detection (LC-OCD-OND) Water Res. 45,
616 879-885.

617 Hudson, N., Baker, A. and Reynolds, D. 2007. Fluorescence analysis of dissolved
618 organic matter in natural, waste and polluted water - a review. River Res Appl.
619 23, 189.

620 Kaza, S., Yao, L., Bhada-Tata, P. and Van Woerden, F. 2018 What a waste 2.0: A
621 global snapshot of solid waste management to 2050. Series, U.D. (ed), World
622 Bank, Washington, D.C.

623 Liu, Q., Schurter, L.M., Muller, C.E., Aloisio, S., Francisco, J.S. and Margerum, D.W.
624 2001. Kinetics and mechanisms of aqueous ozone reactions with bromide,
625 sulfite, hydrogen sulfite, iodide, and nitrite ions. Inorg. Chem. 40, 4436-4442.

626 Miklos, D.B., Remy, C., Jekel, M., Linden, K.G., Drewes, J.E. and Hübner, U. 2018.
627 Evaluation of advanced oxidation processes for water and wastewater treatment
628 - A critical review. Water Res. 139, 118-131.

629 Moreira, F.C., Soler, J., Fonseca, A., Saraiva, I., Boaventura, R.A.R., Brillas, E. and
630 Vilar, V.J.P. 2015. Incorporation of electrochemical advanced oxidation
631 processes in a multistage treatment system for sanitary landfill leachate. Water
632 Res. 81, 375-387.

633 Naumov, S., Mark, G., Jaroki, A. and von Sonntag, C. 2010. The reactions of nitrite
634 ion with ozone in aqueous solution - new experimental data and quantum-
635 chemical considerations. Ozone Sci. Eng. 32, 430-434.

636 Ntampou, X., Zouboulis, A.I. and Samaras, P. 2006. Appropriate combination of
637 physico-chemical methods (coagulation/flocculation and ozonation) for the
638 efficient treatment of landfill leachates. Chemosphere 62(5), 722-730.

639 Oloibiri, V., Chys, M., De Wandel, S., Demeestere, K. and Van Hulle, S.W.H. 2017a.
640 Removal of organic matter and ammonium from landfill leachate through
641 different scenarios: operational cost evaluation in a full-scale case study of a
642 Flemish landfill. J. Environ. Manage. 203, 774-781.

643 Oloibiri, V., Coninck, S., Chys, M., Demeestere, K. and Van Hulle, S.W.H. 2017b.
644 Characterisation of landfill leachate by EEM-PARAFAC-SOM during physical-
645 chemical treatment by coagulationflocculation, activated carbon adsorption and
646 ion exchange. Chemosphere 186, 873-883.

647 Park, M. and Snyder, S.A. 2018. Sample handling and data processing for fluorescent
648 excitation-emission matrix (EEM) of dissolved organic matter (DOM).
649 Chemosphere 193, 530-537.

650 Pastore, C., Barca, E., Del Moro, G., Di Iaconi, C., Loos, M., Singer, H.P. and Mascolo,
651 G. 2018. Comparison of different types of landfill leachate treatment by
652 employment of nontarget screening to identify residual refractory organics and
653 principal component analysis Sci. Total Environ. 635, 984-994.

654 Pluciennik-Koropczuk, E. and Myszograj, S. 2018. Zahn-Wellens test in industrial
655 wastewater biodegradability assessment. Civil and Environmental Engineering
656 Reports 28(1), 77-86.

657 Renou, S., Givaudan, J.G., Poulain, S., Dirassouyan, F. and Moulin, P. 2008. Landfill
658 leachate treatment: review and opportunity. J. Hazard. Mater. 150, 468-493.

659 Rosenfeldt, E.J., Linden, K.G., Canonica, S. and Von Gunten, U. 2006. Comparison of
660 the efficiency of $^{\bullet}OH$ radical formation during ozonation and the advanced
661 oxidation processes O_3/H_2O_2 and UV/H_2O_2. Water Res. 40, 3695-3704.

662 Silva, T.F.C.V., Silva, M.E.F., Cunha-Queda, A.C., Fonseca, A., Saraiva, I., Sousa,
663 M.A., Gonçalves, C., Alpendurada, M.F., Boaventura, R.A.R. and Vilar, V.J.P.
664 2013. Multistage treatment system for raw leachate from sanitary landfill
665 combining biological nitrification-denitrification/solar photo-Fenton/biological

processes, at a scale close to industrial - biodegradability enhancemente and evolution profile of trace pollutants. Water Res. 47, 6167-6186.

Silva, T.F.C.V., Soares, P.A., Manenti, D.R., Fonseca, A., Saraiva, I., Boaventura, R.A.R. and Vilar, V.J.P. 2017. An innovative multistage treatment system for sanitary landfill leachate depuration: Studies at pilot-scale. Sci. Total Environ. 576, 99-117.

Tchobanoglous, G., Burton, F. and Stensel, H. (2003) Wastewater engineering: Treatment and reuse, McGraw-Hill.

Tizaoui, C., Bouselmi, L., Mansouri, L. and Ghrabi, A. 2007. Landfill leachate treatment with ozone and ozone/hydrogen peroxide systems. J. Hazard. Mater. 182, 316-324.

U.S.EPA 1993 Manual - nitrogen control., p. 326, National Service Center for Environmental Publications, USA.

Vedrenne, M., Vasquez-Medrano, R., Prato-Garcia, D., Frontana-Uribe, B.A. and Ibanez, J.G. 2012. Characterization and detoxification of a mature landfill leachate using combined coagulation-flocculation/photo-Fenton treatment. J. Hazard. Mater. 205-206, 208-215.

Vithanage, M., Wijesekara, H., Siriwardana, A.R., Mayakaduwa, S.S. and Ok, Y.S. (2014) Management of municipal solid waste landfill leachate: A global environmental issue, Springer, Netherlands.

Wassink, J.K., Andrews, R.C., Peiris, R.H. and Legge, R.L. 2011. Evaluation of fluorescence excitationemission and LC-OCD as methods of detecting removal of NOM and DBP precursors by enhanced coagulation. Water Supply 11(5), 621-630.

690 Yang, L., Shin, H.S. and Hur, J. 2013. Estimating the concentration and
691 biodegradability of organic matter in 22 wastewater treatment plants using
692 fluorescence excitation emission matrices and parallel factor analysis. Sensors
693 14, 1771-1786.

694 Zhang, D.-B., Wu, X.-G., Wang, Y.-S. and Zhang, H. 2014. Landfill leachate
695 treatment using the sequencing batch biofilm reactor method integrated with the
696 electro-Fenton process. Chemical Papers 68, 782-787.

697

698

699 **Legends**

700 **Figure 1** – Schematics of the experimental setup used for O_3 and O_3/UVC treatment
701 processes.

702 **Figure 2** – Evolution of (a) DOC removal, (b) COD removal, and (c) pH values as a
703 function of treatment time for (.1) O_3 and (.2) O_3/UVC treatments applied to the bio-
704 treated leachates (■, ▬) L_N and (●,▨) L_D, including (×) nitrite and (∗) nitrate
705 concentrations, for L_N.

706 **Figure 3** – (a) Relative fluorescence (▌▌▌▌▌ - regions I to V), (b) 3D-EEM spectra,
707 and (c) SEC-OCD chromatograms ((▬) before and (▬) after O_3/UVC treatment) for
708 the (.1) nitrified leachate – L_N and (.2) nitrified-denitrified leachate – L_D, and after (1'
709 or .2') respective O_3/UVC treatment.. (O_3/UVC treatment conditions: V_L = 1.5 L; Q_{O3} =
710 0.1 L/min; $[O_3]_{inlet}$ = 180 mg/L; ; t = 10h, Q_{UV} = 2.48 J/s).

711 **Figure 4** – Evolution of (a) DOC removal, (b) COD removal, and (c) pH values as a
712 function of treatment time for (.1) O_3 and (.2) O_3/UVC treatments applied to the bio-
713 coagulated leachates (■, ▬) L_N and (●,▨) L_D.

714 **Figure 5** – (a) Relative fluorescence (▌▌▌▌▌ - regions I to V), (b) 3D-EEM spectra,
715 and (c) SEC-OCD chromatograms ((▬) before and after (▬) O_3 and (▬) O_3/UVC
716 treatment) for the (.1) nitrified-coagulated leachate – L_{NC} and (.2) nitrified-denitrified-
717 coagulated leachate – L_{DC}, and after respective (1' or 2') O_3 and (1'' or 2'') O_3/UVC
718 treatment. (coagulation conditions for L_{NC}: $[Fe^{3+}]$ = 240 mg/L and pH ~4; coagulation
719 conditions for L_{DC}: $[Al^{3+}]$ = 300 mg/L and pH = 9.2; O_3 treatment conditions: V_L = 1.5
720 L; Q_{O3} = 0.1 L/min; $[O_3]_{inlet}$ = 180 mg/L; t = 3h; O_3/UVC treatment: same conditions as
721 for O_3, except for Q_{UV} = 1.7 J/s).

722 **Table 1 –** Physicochemical characterization of the landfill leachate after different pre-

723 treatment stages.

Parameter	L_N	L_D	L_{NC}	L_{DC}	ELV[a]
pH	7.5	9.1	3.7	6.2	6.0 – 9.0
DOC[b] (mg/L)	956	1149	430	574	-
DIC[b] (mg/L)	89	464	7	143	-
COD[b] (mg/L)	3479	3577	1174	1635	150
UV_{254} (cm^{-1})	27.1	24.9	6.8	4.1	-
Color[c] (Pt-Co)	320	280	49	26	Not visible
NH_4^+ (mg N/L)	< 0.1	< 0.1	< 0.1	< 0.1	8
NO_2^- (mg N/L)	1034	< 0.1	< 0.1	< 0.1	-
NO_3^- (mg N/L)	19	14	523	12	10
Cl^- (mg/L)	2723	2480	2639	2630	-
SO_4^{2-} (mg/L)	247	319	1721	1903	2000
Al (mg/L)	1.8	2.0	2.2	2.4	10
Cr (mg/L)	1.5	1.2	0.7	< 0.08	2.0
Cu (mg/L)	< 0.01	< 0.01	0.3	0.4	1.0
Fe (mg/L)	5.3	3.0	12.6	0.3	2.0
Ni (mg/L)	n.d.	n.d.	< 0.25	< 0.25	2.0
Pb (mg/L)	< 0.25	< 0.25	< 0.25	< 0.25	1.0
Biodegradability (%)	7	18	17	19	-

724 [a] Emission limit values (ELV) in Portugal for the discharge of wastewaters in receiving water bodies
725 (Decree-Law no 236/98).
726 [b] DOC – dissolved organic carbon; DIC – dissolved inorganic carbon; COD – chemical oxygen demand.
727 [c] Diluted 1:20.

728 **Table 2 –** Main results and kinetic parameters, for DOC and COD degradation, of the O_3 and O_3/UVC processes applied to bio-treated (L_N and
729 L_D) and bio-coagulated (L_{NC} and L_{DC}) leachates.

Parameters	O_3			O_3/UVC		O_3		O_3/UVC	
	L_N	L_D		L_N	L_D	L_{NC}	L_{DC}	L_{NC}	L_{DC}
OD_I [a] (g O_3/L)	8.6	8.6		7.2	7.4	2.2	2.1	2.2	2.2
OD_T [a] (g O_3/L)	8.0	7.9		7.1	7.1	1.8	1.5	2.1	2.1
DOC removal (%)	50.5	49.3		73.2	62.9	36.2	26.1	54.5	43.3
COD removal (%)	64.8	68.7		79.4	82.9	53.1	36.4	69.9	60.0
Color removal (%)	93.7	89.4		97.8	93.1	69.3	62.2	77.6	70.2
Biodegradability (%)	51	69		73	80	81	83	93	87
	DOC Degradation Kinetics								
k [b]$\times 10^3$ (min^{-1})	2.0 ± 0.1	1.2 ± 0.1		4.7 ± 0.9	1.9 ± 0.2	2.5 ± 0.2	1.9 ± 0.2	4.2 ± 0.4	3.6 ± 0.4
R^2 [c]	0.997	0.995		0.990	0.994	0.996	0.996	0.991	0.992
t [d] (min)	> 420	> 240		> 360	> 120	> 0	> 60	> 30	> 30
k [e]$\times 10^{-1}$ (mg DOC/g OD_T)	12.0 ± 0.9	8.5 ± 0.5		19 ± 1	10.4 ± 0.7	7.8 ± 0.8	8.4 ± 0.6	11.8 ± 0.8	12.7 ± 0.9
R^2 [c]	0.997	0.997		0.997	0.994	0.994	0.996	0.995	0.994
OD_T [d] (g O_3/L)	> 5.0	> 2.9		> 3.6	> 0	> 0	> 0	> 0.2	> 0.2
	COD Degradation Kinetics								
k [b]$\times 10^3$ (min^{-1})	1.7 ± 0.1	1.60 ± 0.08		2.7 ± 0.4	2.7 ± 0.2	4.2 ± 0.8	2.1 ± 0.4	6.5 ± 0.8	5.1 ± 0.5
R^2 [c]	0.991	0.994		0.994	0.995	0.990	0.991	0.993	0.996
t [d] (min)	> 120	> 0		> 0	> 0	> 0	> 0	> 0	> 0
k [e]$\times 10^{-2}$ (mg COD/g OD_T)	3.0 ± 0.2	4.0 ± 0.3	2.2 ± 0.2	3.7 ± 0.2	2.7 ± 0.1	3.4 ± 0.6	3.3 ± 0.5	4.0 ± 0.6	4.6 ± 0.8
R^2 [c]	0.994	0.997	0.994	0.998	0.998	0.996	0.993	0.995	0.991
OD_T [d] (g O_3/L)	> 0	< 3.6	> 3.6	> 0	> 1.4	> 0	> 0	> 0	> 0

730 [a] Inlet (OD_I) and transferred (OD_T) ozone dose per liter of leachate.
731 [b] Pseudo-first-order rate constant for DOC and COD degradation in terms of reaction time.
732 [c] Coefficient of determination.
733 [d] Value or interval of time (t, min) or transferred ozone dose (OD_T), from which the kinetic parameters were calculated.
734 [e] DOC and COD degradation reaction rates, expressed in terms of the transferred ozone dose (OD_T), whose values correspond to the slopes of Fig. SM-1 (a.1) and (b.1), for
735 L_N and L_D, and of Fig. SM-4 (a.1) and (b.1), for L_{NC} and L_{DC}.

736 **Table 3** – Operating costs estimation for the different treatment train strategies.

			Treatment train					
		Un	**Bio_{NIT} + O_3/UVC + Bio_{DESN}**	**$Bio_{NIT/DESN}$ + O_3/UVC + $Bio_{OXID.}$**	**Bio_{NIT} + C/S + O_3 + Bio_{DESN}**	**Bio_{NIT} + C/S + O_3/UVC + Bio_{DESN}**	**$Bio_{NIT/DESN}$ + C/S + O_3 + Bio_{OXID}**	**$Bio_{NIT/DESN}$ + C/S + O_3/UVC + Bio_{OXID}**
1st Bio.[a]	Aeration	€/m^3	0.10	0.10	0.10	0.10	0.10	0.10
	Methanol	€/m^3	-	0.57	-	-	0.57	0.57
	(1) TOTAL	**€/m^3**	**0.10**	**0.67**	**0.10**	**0.10**	**0.67**	**0.67**
Coagulation[b]	H_2SO_4	€/m^3	-	-	0.08	0.08	-	-
	$FeCl_3$	€/m^3	-	-	0.42	0.42	-	-
	$Al_2(SO_4)_3$	€/m^3	-	-	-	-	0.75	0.75
	Sludge	€/m^3	-	-	0.48	0.48	0.48	0.48
	(2) TOTAL	**€/m^3**	**-**	**-**	**0.98**	**0.98**	**1.23**	**1.23**
O_3-driven[c]	NaOH	€/m^3	0.18	-	0.43	0.34	0.50	0.28
	O_2	€/m^3	4.07	3.75	1.16	0.78	1.95	0.96
	Energy	€/m^3	29.4	27.1	5.01	4.58	8.42	5.65
	(3) TOTAL	**€/m^3**	**33.7**	**30.8**	**6.61**	**5.69**	**10.88**	**6.89**
2nd Bio.[d]	Aeration	€/m^3	0.03	0.06	0.03	0.03	0.06	0.06
	Methanol	€/m^3	0.86	-	0.81	0.81	-	-
	(4) TOTAL	**€/m^3**	**0.89**	**0.06**	**0.84**	**0.84**	**0.06**	**0.06**
(1) + (2) + (3) + (4)			**34.6**	**31.6**	**8.5**	**7.6**	**12.8**	**8.6**

737 [a] The following theoretical values were assumed: 3.43 kg O_2 consumed per kg N-NO_2^- formed (for nitritation) and 1.72 kg COD consumed per kg N-NO_2^- reduced (for denitritation).

738 [b] Conditions: 240 mg Fe^{3+}/L, pH ~ 4, requiring 0.42 L of H_2SO_4 per m^3 of bio-nitrified leachate; and 300 mg Al^{3+}/L without pH adjustment, for the nitrified/denitrified leachate.

739 [c] Conditions: initial pH adjusted to 9.0; Q_g = 0.1 L/min; $C_{O_3,I}$ = 180 mg O_3/L.

740 [d] The following theoretical value was assumed: 2.89 kg COD per g N-NO_3^- reduced (for denitrification).

Figure 1

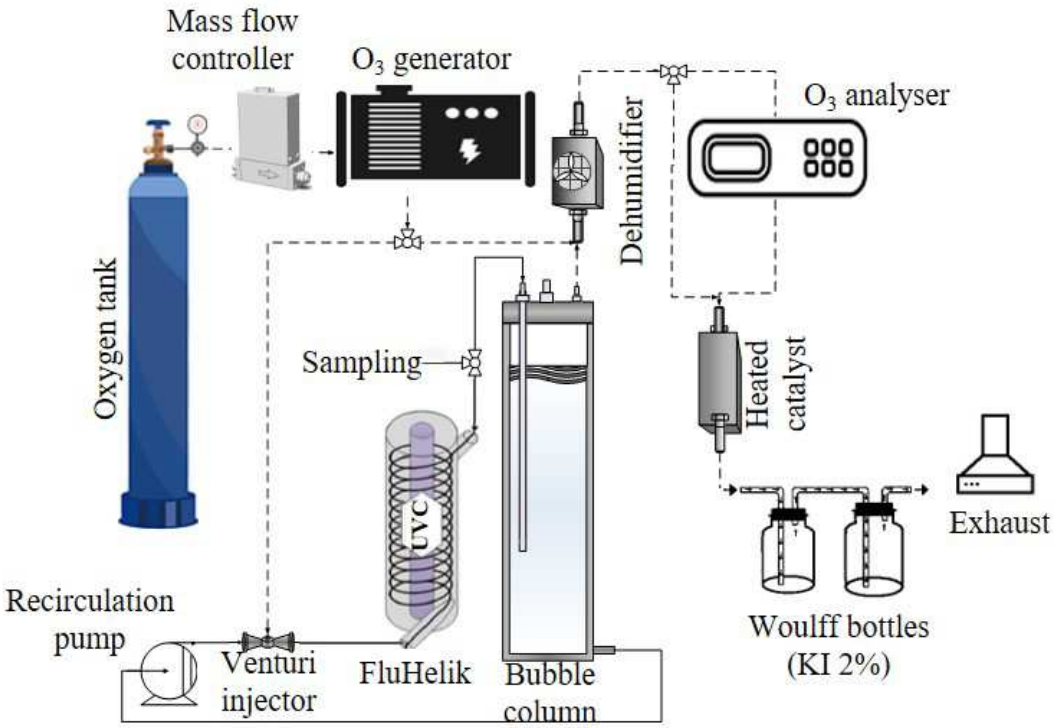
Mass flow controller
O_3 generator
O_3 analyser
Dehumidifier
Oxygen tank
Sampling
Heated catalyst
UVC
Exhaust
Recirculation pump
Venturi injector
FluHelik
Bubble column
Woulff bottles (KI 2%)

Figure 2

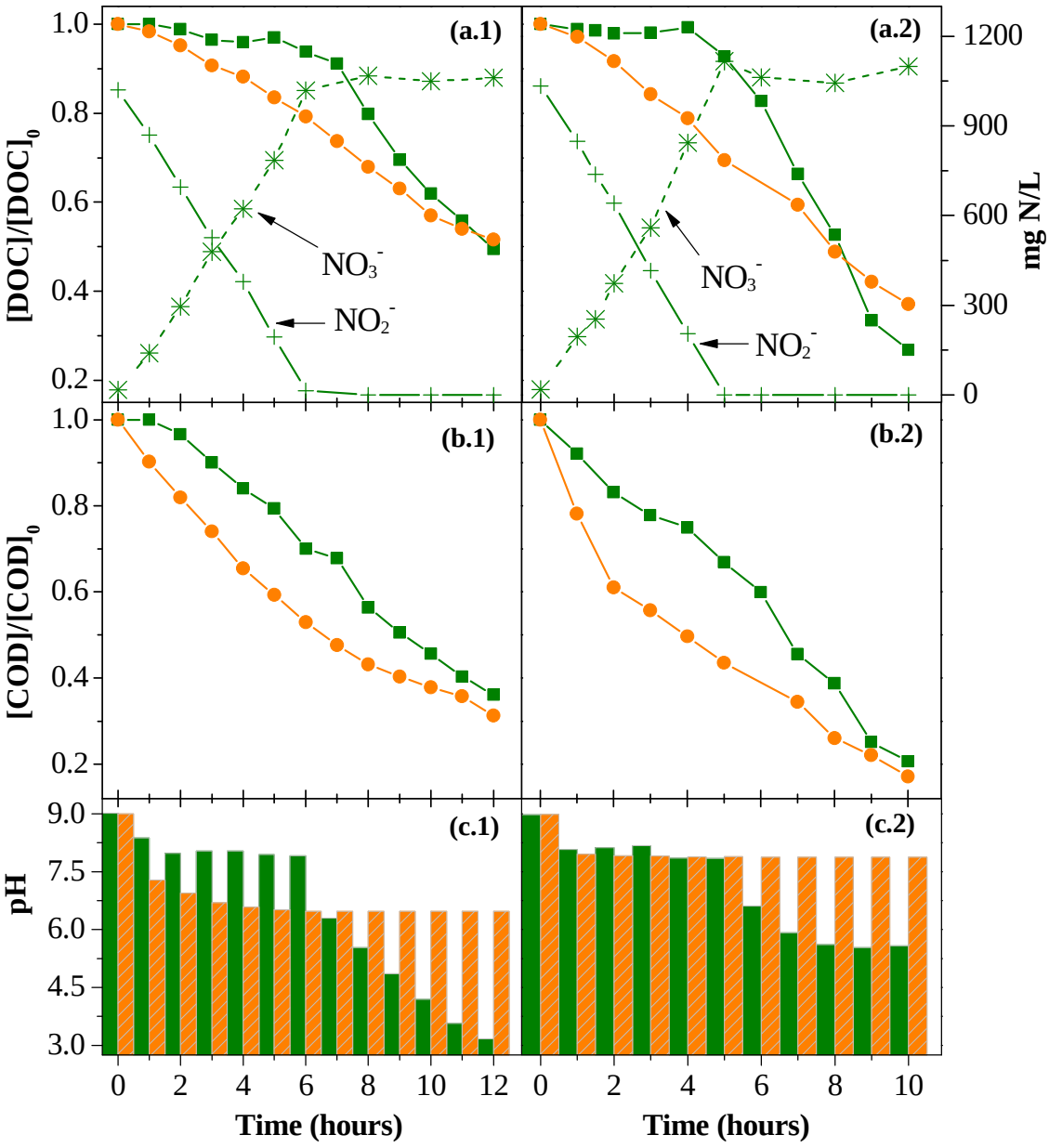
(a.1)
(a.2)
(b.1)
(b.2)
(c.1)
(c.2)
[DOC]/[DOC]0
[COD]/[COD]0
pH
mg N/L
NO3-
NO2-
Time (hours)
Time (hours)

Figure 3

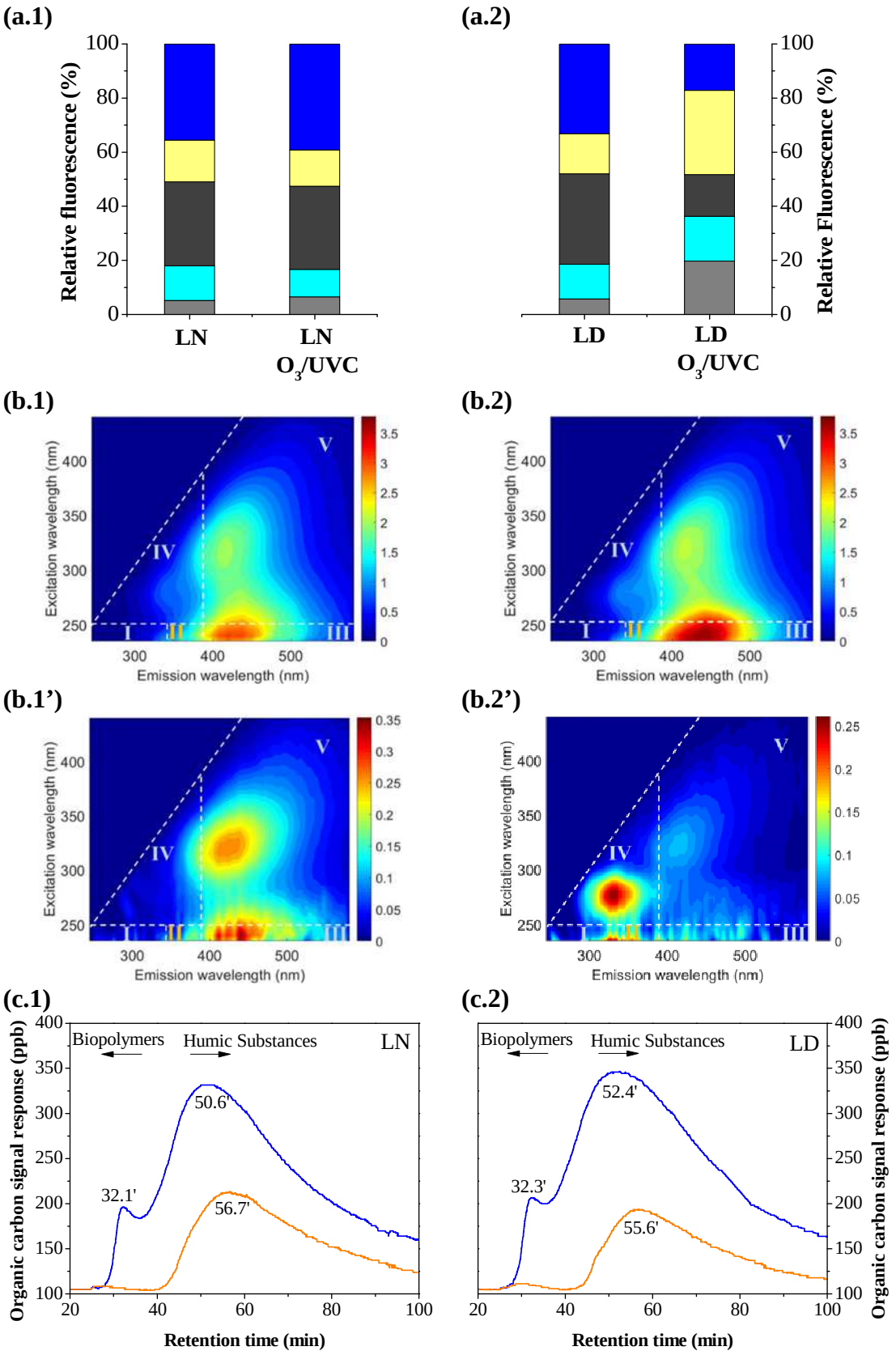
(a.1)
Relative fluorescence (%)
LN
LN O3/UVC
(a.2)
Relative Fluorescence (%)
LD
LD O3/UVC
(b.1)
(b.2)
(b.1')
(b.2')
Excitation wavelength (nm)
Emission wavelength (nm)
I
II
III
IV
V
(c.1)
(c.2)
Organic carbon signal response (ppb)
Retention time (min)
Biopolymers
Humic Substances
LN
LD
50.6'
32.1'
56.7'
52.4'
32.3'
55.6'

Figure 4

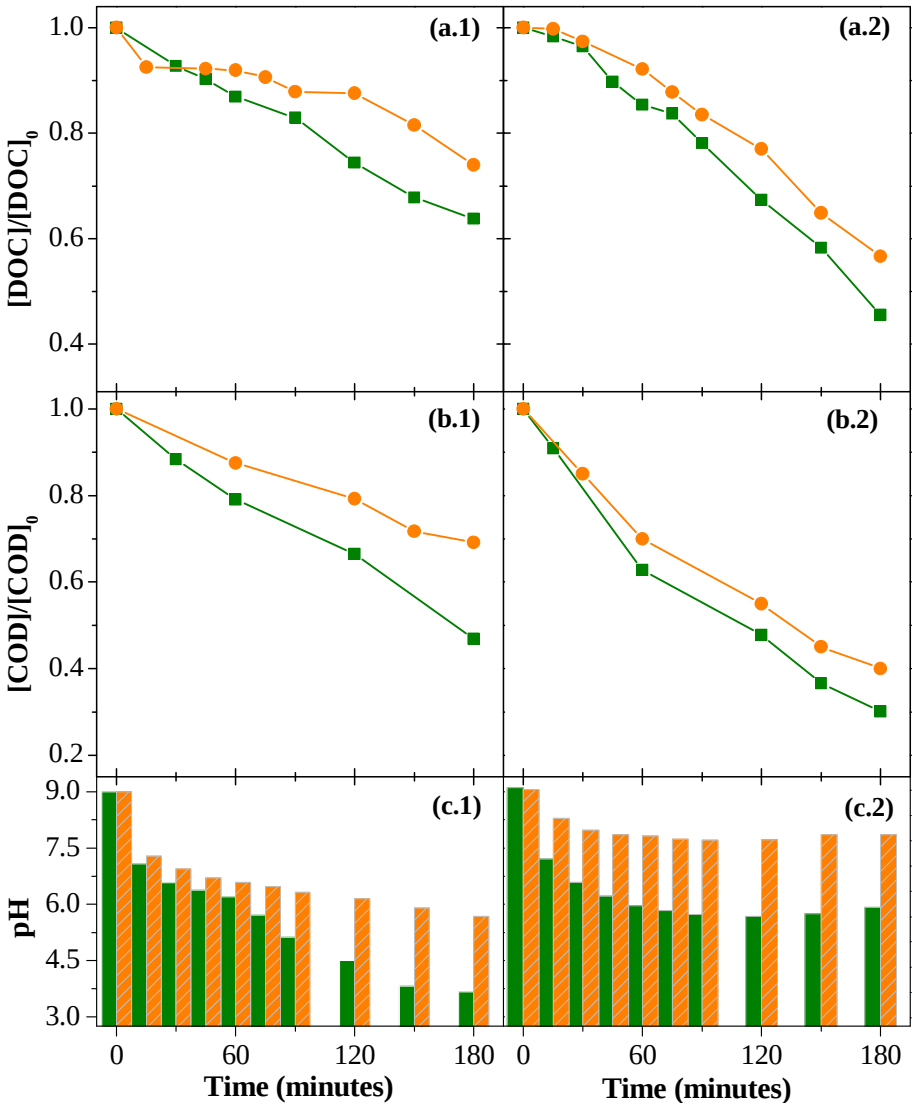
(a.1)
(a.2)
(b.1)
(b.2)
(c.1)
(c.2)
[DOC]/[DOC]0
[COD]/[COD]0
pH
1.0
0.8
0.6
0.4
0.2
9.0
7.5
6.0
4.5
3.0
0
60
120
180
Time (minutes)
Time (minutes)

Figure 5

(a.1) **(a.2)**

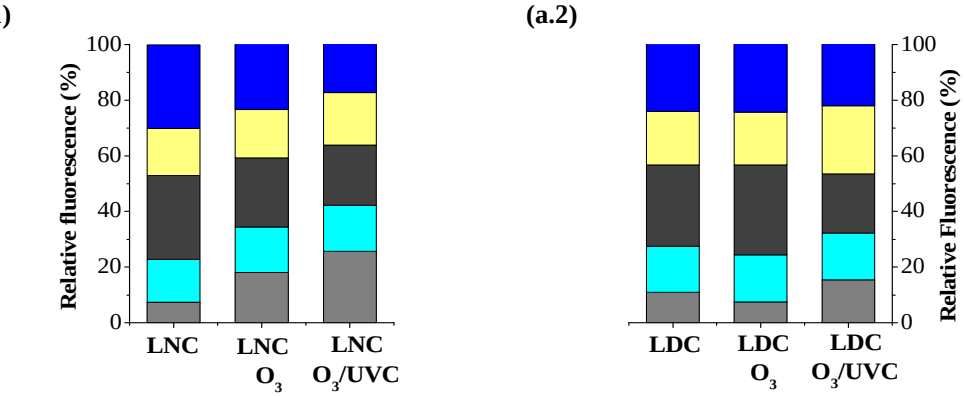

(b.1) **(b.2)**

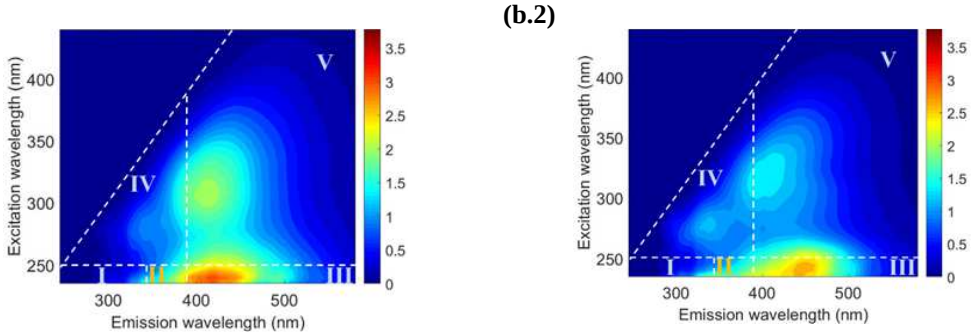

(b.1') **(b.2´)**

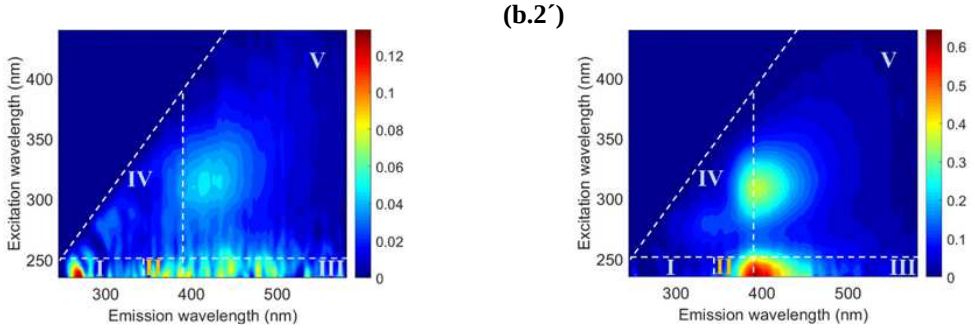

(b.1'') **(b.2'')**

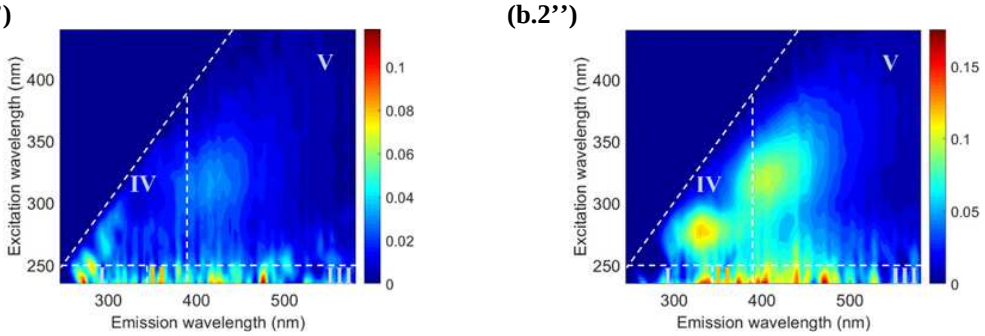

(c.1) **(c.2)**

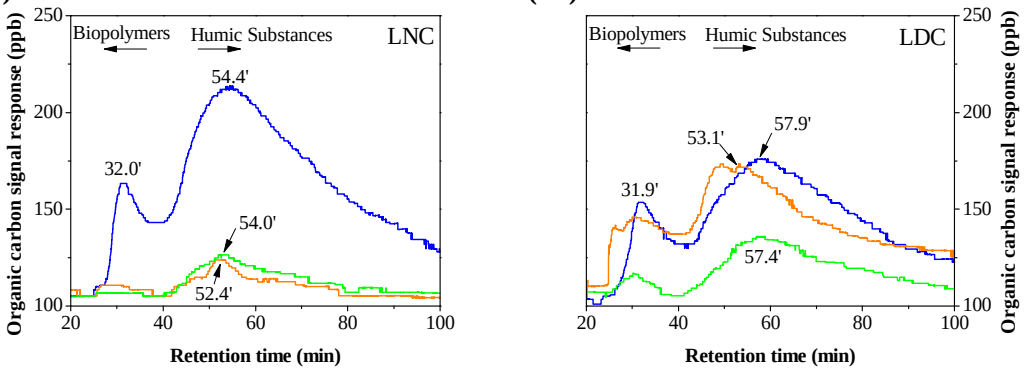

Highlights

- Fast O_3 use to oxidize NO_2^- of the nitrified-leachate, thus hindering DOC decay.

- Coagulation selectively removed high molecular weight humic matter.

- Treatment train able to reach COD <150 mg/L, TN <15 mg/L and SO_4^{2-} <2000 mg/L.

- O_3/UVC applied to L_{DC} represents 77.5% of the total operating cost (8.9 €/m^3).

Declaration of interests

☒ The authors declare that they have no known competing financial interests or personal relationships that could have appeared to influence the work reported in this paper.

☐The authors declare the following financial interests/personal relationships which may be considered as potential competing interests: